ANTHROPOLOGIE • XLVIII/2 • pp. 163–176 • 2010

DORIS SCHAMALL, MARIA TESCHLER-NICOLA

OSTEOMALACIC MICROARCHITECTURE EXEMPLIFIED BY A LATE ANTIQUITY SKELETON AND VERIFIED BY BSE-MODE IN A SEM

ABSTRACT: Although rickets and osteomalacia have already been reported in archeological contexts and more recently have become a subject of increased interest, there are just a few of them approved by histological investigation. Here we present the results of a study carried out on the skeletal remains of a female recovered from Linz, Austria, dated to the Late Antiquity. Previous macroscopic inspection yielded pathological features which implied an osteomalacic origin. To verify this assumption we compared this specimen with a fluid-conserved historical vertebra with documented osteomalacia from the collection of the Federal Pathologic-Anatomical Museum (PAM) in Vienna; for this purpose, non-invasive radiological and invasive histological examinations, specifically the most promising, scanning electron microscope (SEM) inspection in backscattered electron-mode (BSE-mode) was used. This approach revealed not only the reliability of the BSE-mode technique for identifying such disorders in earth-stored ancient skeletal remains, but it also demonstrated its potential for distinguishing between disturbed bone-mineralization and taphonomic changes. We further ascertained criteria conducive to differential diagnosis of osteomalacia based on trabecular configuration and mineralization status of vertebral bodies.

KEY WORDS: Osteomalacic bone microarchitecture – X-ray-, histological-, and SEM technique – Late Antiquity – Austria

INTRODUCTION

Bone is a dynamic tissue that ensures not only the mechanical integrity of the body, but is also significantly involved in the homeostasis of minerals (Stout 1989, Einhorn 1996, Kamboi 2007). For the sustainability of metabolic processes, a specific concentration of mineral salts is required and their constant ionic levels are controlled and regulated by vitamins and hormones. An alteration of one of these factors, either due to malnutrition, insufficient organ function, disturbed metabolism, intoxication, disease, or a combination of these causes may lead to impairment or even deficiency of bone tissue associated organs. For example, vitamin D is responsible for the mineralization of the organic bone matrix (osteoid) and homeostatic maintenance. This process requires a constant level of calcium and phosphorus in the blood serum and with it a well-balanced mobilization of these minerals. A lack of vitamin D is followed by a decrease of the intestinal calcium absorption and subsequently leads to diminished calcium transfer between blood and bone, finally resulting in skeletal changes such as rickets in subadults or osteomalacia in adults (Jaffe 1972, Revell 1986, Pitt 1995, Löffler, Petrides 2003).

Rickets and osteomalacia have not been frequently documented in archeological contexts, nor do many systematic population studies exist (Mays 2003, Brickley *et al.* 2005). Nevertheless, some cases are reported from the Neolithic, Roman times, and the Middle Ages (e.g., Ruffer 1911, Sigerist 1951, Wells 1964, Zivanovic 1982,

FIGURE 1. a) Linz, grave No. 22, female (aged 35–45 years). Macroscopic view of the left proximal humerus – note common fracture healed in angular malposition; b) note the right scapula fragment with complete and incomplete fractures; c) note the proximal portion of the left fractured ulna and the right ulna exhibiting a cortical fissure; d) note the ischial ramus from the right pelvis with fractures, but without deformations; e) note the costae with pseudofractures (PF); one with a callus (CL); f) note the left metatarsal bone with a healed fracture; g) note the left tibia with subperiosteal appositions of newly built bone.

Molleson 1988, Molleson, Cox 1993 Stuart-Macadam 1989, Formicola 1995, Carli-Thiele 1996, Ortner, Mays 1998, Aufderheide, Rodríguez-Martin 1998, Roberts, Cox 2003, Ortner 2003, Roberts, Manchester 2005). Most often the diagnosis was compiled by macroscopic inspection and radiographic techniques alone.

During a systematic paleopathological screening of 38 individuals recovered from a Late Antiquity (4th–6th century AD) burial site at Linz (Upper Austria), the fragmentary skeleton of a female with extremely light long bones, a remarkable reduction of the cortical bone thickness, several fractures, and unusual cortical fissures was identified by using conventional methods (Wiltschke-Schrotta, Teschler-Nicola 1991). Based on these features, osteomalacia was assumed. Following the successful implementation of invasive histological techniques for differential diagnostic purposes in recent clinical cases of osteomalacia (Boyde *et al.* 1986), Teschler-Nicola *et al.* (1996) applied the

backscattered electron-mode (BSE-mode) in a scanning electron microscope (SEM) for the first time to investigate an ancient case.

Here we aim to re-investigate this case a) in order to verify and discuss the previous diagnosis by comparing the Late Antiquity specimen with a fluid-conserved vertebra from the 19th century with documented osteomalacia (the latter was provided from the collection of historical skeletal remains of the Federal Pathologic-anatomical Museum in Vienna) and b) to ascertain criteria conducive to a diagnosis of osteomalacia based on trabecular configuration and mineralization status of vertebral bodies. We further intended to identify taphonomic changes.

MATERIALS AND METHODS

We investigated skeletal remains recovered from a Late Antiquity burial site in Linz, Upper Austria (Tiefer Graben, Flügelhofgasse, grave No. 22) characterized by several pathological features. The preservation status was quite poor, but main portions of all skeletal elements were preserved: the calotte and the cranial base, fragments of the facial skeleton and several teeth, parts of the axial skeleton (vertebrae), shoulder girdle, two small fragments of the right pelvis, several remnants of the lower and upper limb bones, feet and hand bones. Age-at-death and sex estimations were determined using conventional anthropological methods (Acsádi, Nemeskéri 1970, Ferembach *et al.* 1979, Sjøvold 1988, Işcan, Kennedy 1989, Biukstra, Ubelaker 1994). Nearly all morphological features were indicative of a female. Despite the occurrence of conspicuous alterations, an age-of-death between 35 and 45 years was plausible.

In addition to the gross-anatomical examination (photographically documented by a NIKON F90, Nikon Corp., Tokyo, Japan) and radiological evaluation (PRACTIX 33 P1-013, Philips, Best, The Netherlands), a microscopical investigation was carried out. As conventional preparation of decalcified microtome sections was not applicable to the porous and fragile remains, undecalcified sections of selected bone samples – fragments of the right scapula, a lumbar vertebra, a portion of the left distal tibia, and the left second metatarsal bone – were resin-embedded in poly-methyl-methacrylate (PMMA; Plenk jr. 1989). After hardening, blocks were cut, fixed on microscope slides, polished, and carbon-sputtered for investigation in a SEM (ZEISS DSM 692, Oberkochen, Germany) in the BSE-mode using a 4-quadrant semiconductor BSE detector. Depending on the atomic number of the chemical elements present, the signals are converted in gray scale images that reflect the mineral density distribution due to differences in the mean atomic number (Boyde *et al.* 1986, Bell, Jones 1991, Roschger *et al.* 1995).

Additionally, a fluid-conserved third lumbar vertebra from a documented 65 year old osteomalacic female – stored at the Federal Pathologic-Anatomical Museum (PAM) – was examined for comparative purpose. We used the same techniques described above. This specimen belongs to the collection of historical vertebrae at the PAM (attributable to the end of the 19th century); its individual parameters and pathologic-anatomic data are documented in the inventory register (Schamall *et al.* 2002, 2003a, 2008).

RESULTS

Macroscopic analysis

As previously mentioned, several elements of the Late Antiquity skeleton were not only extremely light, but exhibited also multiple healed and unhealed fractures and fissures: for example, the proximal portion of the left humerus showed a common two-part fracture, where the fragments were displaced against each other, building an angular malposition (*Figure 1a*). A bony callus implies normal healing. As there was still prominent bone formation we concluded that the injury occurred approximately three months before death. Proximally to the fracture, the cortical layer was considerably diminished. Another common fracture with new bone formation was observed at the distal end of the left radius.

On the right scapula, represented by a small central portion, four complete and incomplete fractures were found. The complete fractures were localized at a) the axillary border, three cms below the glenoid cavity and b) the apex of the acromion process; the incomplete fractures were found at a) the basis of the acromion process and b) the scapular spine (*Figure 1b*). The right ulna showed a medial cortical fissure close to the coronoid process and a second (complete) disconnection distally, approximately three cms above the wrist. The fracture breaking edge was covered by irregular, spongy-like and undulating structures. A similar appearance occurred at the proximal left ulna, located approximately between the dia- and metaphysis. Although the coronoid process of the left ulna was not preserved, a complete disconnection can be assumed (*Figure 1c*). Several small and poorly preserved pelvic fragments were featured with the same type of complete spontaneous disconnections. We found them e.g., beneath the acetabular cavity and at the junction between pubic and ischial bone (*Figure 1d*). Furthermore, several ribs (*Figure 1e*) and the diaphysis of the left second metatarsal bone were affected as well and characterized by a spindle-shaped callus. Although a small fracture line remained at the latter, healing had already proceeded (*Figure 1f*).

Beyond these many complete and incomplete, healed and unhealed fractures, there were a few skeletal elements, such as the tibia, showing subperiosteal apposition of newly built bone (*Figure 1g*). Interestingly, the preserved vertebral fragments did not show any irregularities except for moderate impressions at the endplates. In this regard, the Late Antiquity and control sample differ noticeably (*Figure 5a*). The latter revealed a more accentuated impression at both endplates and Schmorl's nodes – herniae that intruded from the disci intervertebrales and compressed the vertebral

FIGURE 2. a) Linz, grave No. 22, female (aged 35–45 years). X-ray of the left proximal humerus; b) X-ray of the right scapula; c) X-ray of the right and left ulna; d) X-ray of the ischial ramus from the right pelvis; e) X-ray of a costa; f) X-ray of the left metatarsal bone; g) X-ray of the left tibia near the distal joint; h) X-ray in transversal projection of the middle and distal carpal phalanx from the Late Antiquity specimen – note the absence of subperiosteal erosions that excludes the presence of sHPT.

body to a biconcave shape. However, this result was not surprising, if the advanced age of the control individual is taken into account.

X-Ray analysis

X-ray images (*Figures 2a–g*) of the Late Antiquity skeletal elements showed a visible reduction of radiodensity in general. Additionally, the trabecular structures appeared "coarsened" and the cortical bone was considerably thinned.

All the fractures identified macroscopically were also traceable radiologically: the (common) humerus fracture impressed by its conspicuous distortion and callus formation. The others were characterized either by a cortical disruption or a complete fragmentation without signs of healing (often occurring bilaterally and horizontally to the axis in long bones). This form of partitioning, in particular the incomplete one, may easily be macroscopically overlooked in taphonomically altered skeletal remains. However, by X-ray inspection the affected areas appeared as small "double-lined" dense zones primarily localized in mechanically stressed regions (e.g., at the scapula and pelvic bone, and at the radius and ulna of the Late Antiquity case).

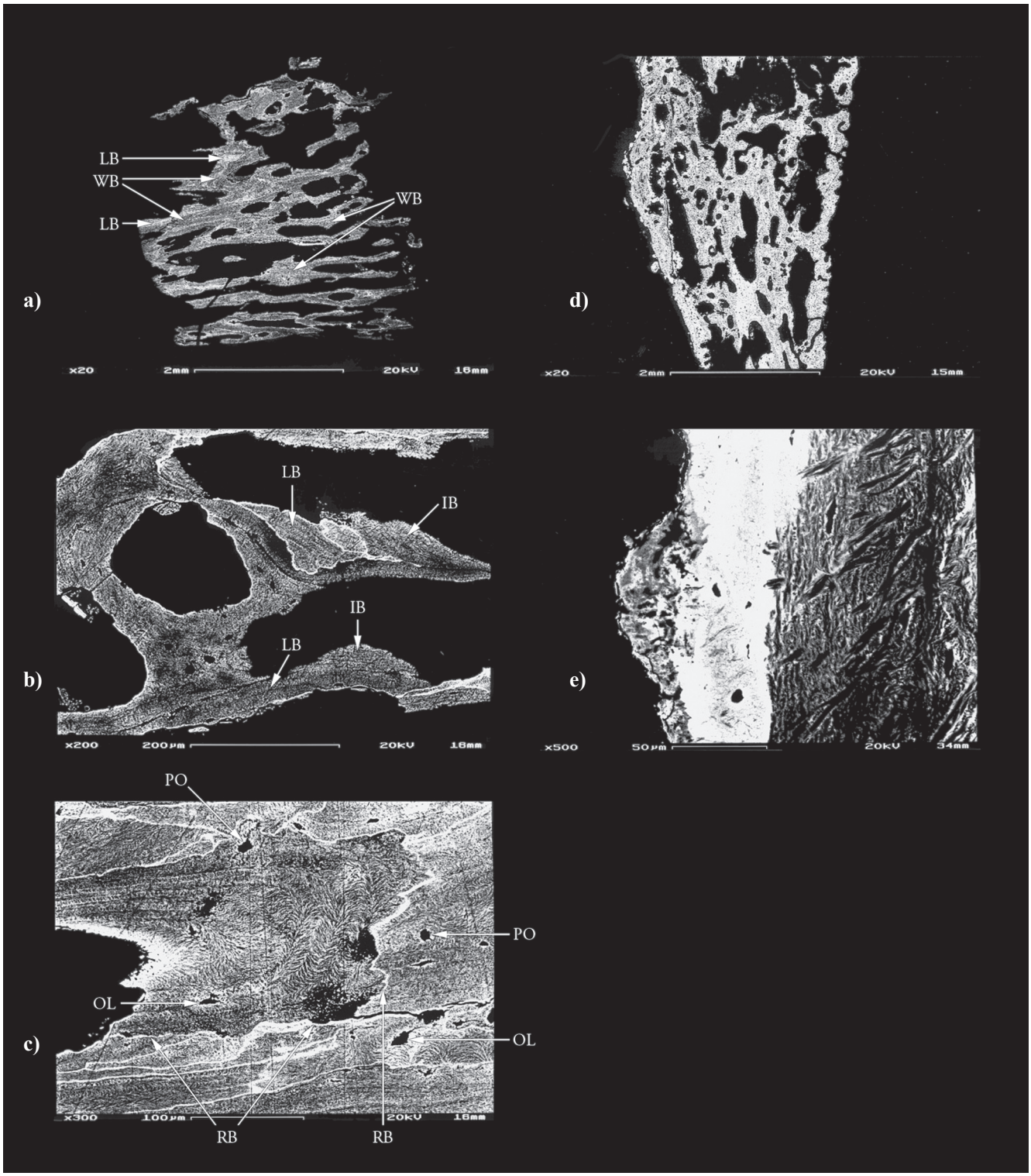

FIGURE 3. a) Linz, grave No. 22, female (aged 35–45 years). BSE- image of the surface of a PMMA-embedded scapula sample (×20) – note plexiform bone structures that consist of woven bone (WB) in the center of each layer which is surrounded by newly formed lamellar bone (LB); b) Detail of *Figure 3a* (×200) – note that lamellar bone (LB) has been resorbed at multiple locations and has been commonly replaced by rapidly assembled immature forms of bone (IB) which is defectively mineralized; c) detail of *Figure 3a* (×300) – note the disturbed mineralization with widened resorptive borders (RB), osteocyte lacunae (OL), and primary osteons (PO); d) BSE-image of the surface of a PMMA-embedded tibia sample (×20) – note the decomposition from compact into spongy bone; e) detail of *Figure 3d* (×500) – note periosteal reaction expressed by newly built deposits.

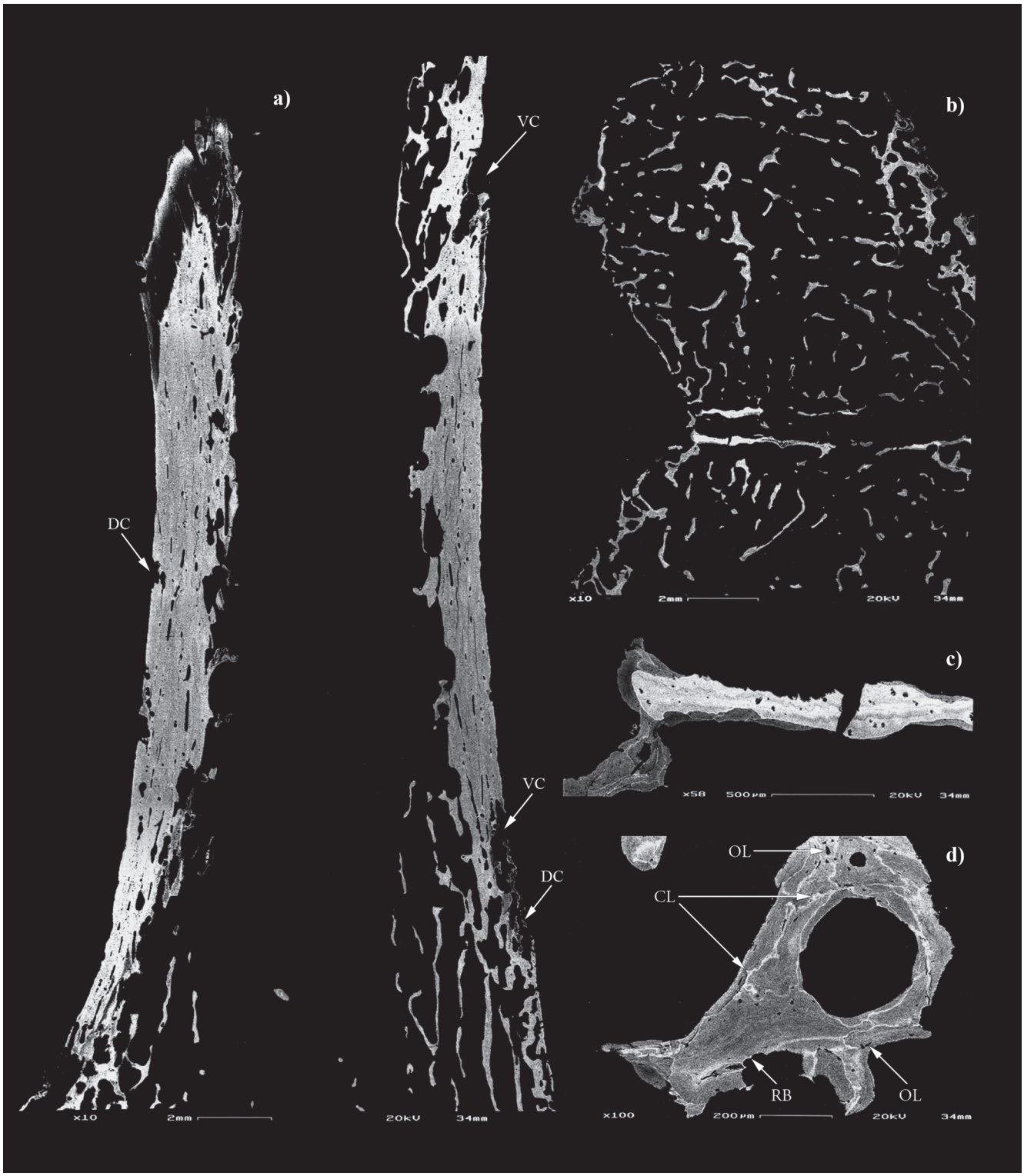

FIGURE 4. a) Linz, grave No. 22, female (aged 35–45 years). BSE-image of the surface of a PMMA-embedded metatarsal bone sample (×10) – the mounting of 5 images demonstrates the course of development of regular to pathologically altered bone; note the vascular channels (VC) in comparison to decompositions (DC); b) BSE-image of the surface of a PMMA-embedded vertebra sample (×10) – the mounting of 2 images reveals the presence of spongy bone in the areas of cortical bone; c) detail of *Figure 4b* (×58) – note differentially mineralized regions within a trabecula, faded borders at its margins, and a disconnection; d) detail of *Figure 4b* (×100) – note irregularly arranged cement lines (CL), enlarged resorptive borders (RB), and osteocyte lacunae (OL).

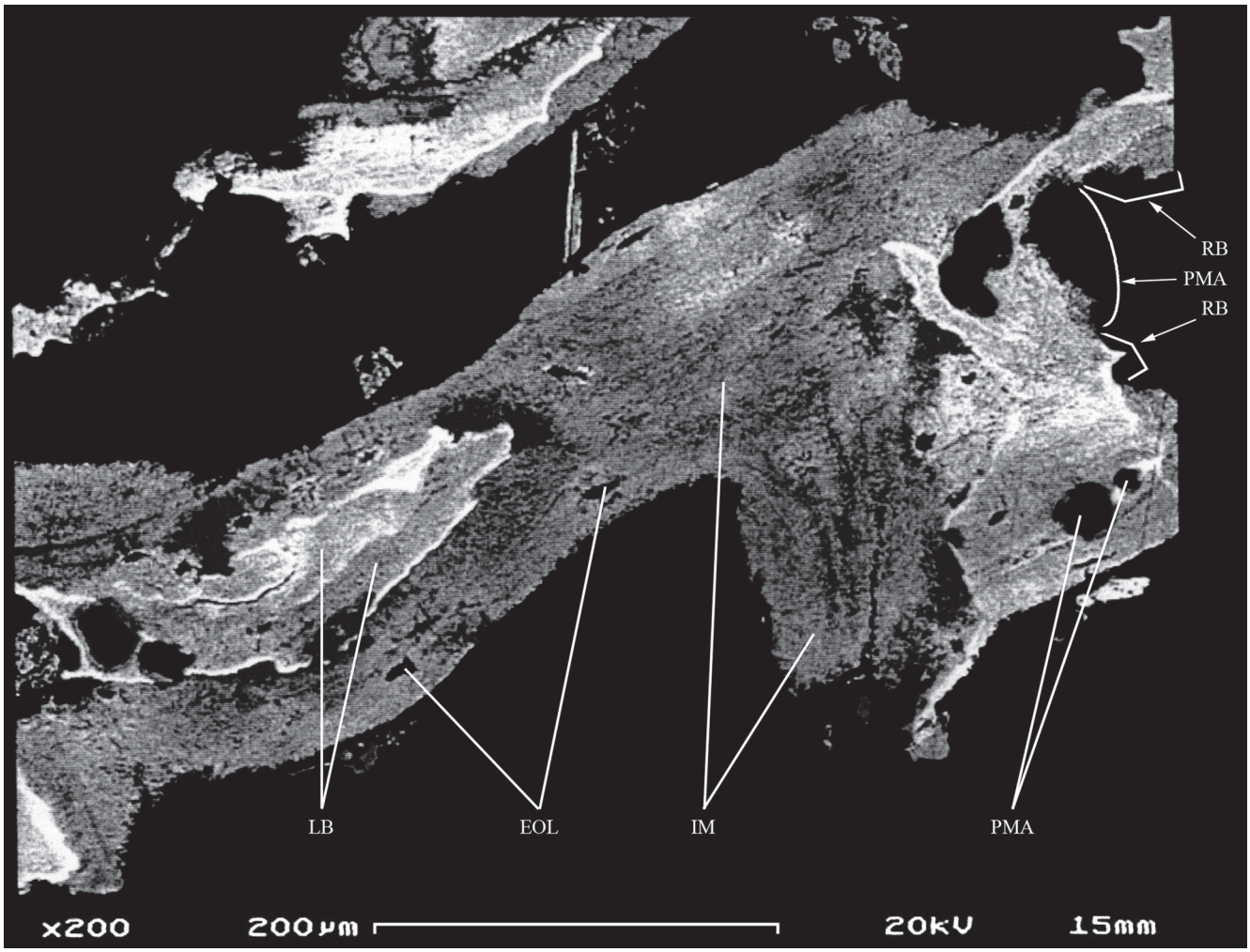

FIGURE 4. e) detail of *Figure 4b* (×200) – although poor preservation status and post-mortem alterations (PMA), the modified portion of the mineralized bone is visible: besides lamellar bone (LB) also inadequate mineralization (IM) occurs. Note resorptive borders (RB) and enlarged osteocyte lacunae (EOL).

A slight reduction of radiodensity, "coarsened" trabeculae, and a thinned cortical bone was also found in the fluid-conserved historical vertebral body (*Figure 5b*). But this item differed by it's broad osteosclerotic zone formed close to the endplates as well as a resorption of structures within the central region.

BSE-mode analysis

Images obtained by this method revealed, even at low magnification, plexiform bone structures. The sample from the right scapula of the Late Antiquity specimen (*Figure 3a*) was taken from the fracture at the axillary margin, three cms below the cavitas glenoidalis. Only a few, light gray layers of woven bone in the center of the trabeculae were found, surrounded by thick layers of newly formed, dark gray lamellar bone. Another scapular region (*Figure 3b*) exhibited predominantly irregularly arranged bone tissue. A detail from this field of view impressed by an extended resorptive border at one trabecular edge (image border below), but only a diffuse appearance along the margin. In higher magnification (*Figure 3c*) the degree of disturbed mineralization is indicated by different levels of gray, primary osteons without cement lines, and enlarged osteocyte lacunae.

By inspection of the tibial shaft sample (*Figure 3d*) we recognized cortical thickening at the periosteal side caused by superficial "porotic" layers of newly built bone. The newly built deposits of the outermost layer was poorly mineralized as indicated by the dark gray appearance (*Figure 3e*). The bright gray layer underneath represents a higher degree of calcification rather than a post-mortem effect.

The mounting of five fields of view to one overview of the fractured metatarsal bone (*Figure 4a*) showed a mainly regularly configured diaphysis. Adjacent to the callus formation, the cortical layers were modified both periosteally and endosteally. Externally, the newly built bone appositions are corresponding to the structures observed at the tibia (see *Figures 3d* and *3e*). Internally, longitudinally oriented newly build bone layers are dominating (*Figure 4a*).

The examination of a lumbar vertebral body fragment revealed a pronounced remodeling at the cortical layer by

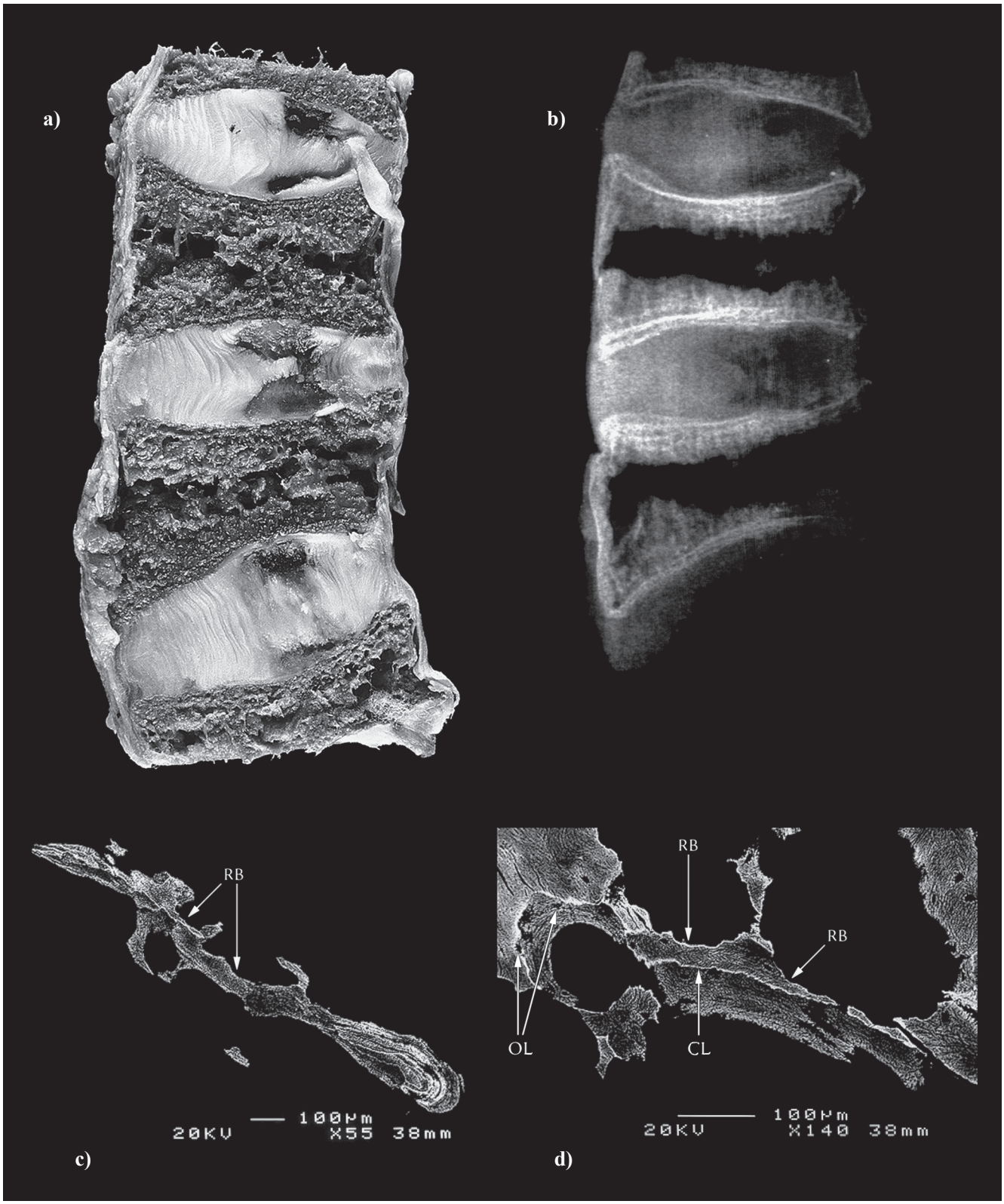

FIGURE 5. a) Fluid-conserved 3rd and 4th lumbar vertebra from a 65 years old osteomalacic female. The lateral view reveals "fish-shaped vertebrae"; b) X-ray in lateral projection from the same vertebrae – note the reduction of radiodensity, the "coarsened" trabecular pattern, and the broad osteosclerotic close to the endplates; c) BSE-image of the surface of a PMMA-embedded ground section of the 3rd lumbar vertebra from the same historical individual (×55) – note the differently mineralized areas within a trabecula and unusual resorption borders (RB); d) BSE-image of another detail of the same 3rd lumbar vertebra (×140) – note conspicuous cement lines (CM) as well as irregularly formed and mineralized trabeculae with enlarged osteocyte lacunae (OL) and resorptive borders (RB).

disaggregation of the compact bone and a small outgrowth at the upper end of the side wall; although localized in the cortical area, it had a cancellous character. The number of trabeculae in the spongy tissue was reduced and the cancellous portions were thinned and even partly disconnected (*Figure 4b*, a mounting of two fields of view). In the center of the vertebral body, different gray colored layers suggested varying mineralization degrees. The upper edge of a trabecula selected from this region reflected this finding and an increased osteoclastic activity impressively. The latter was substantiated by many confluent resorption lacunae (*Figure 4c*). In addition to the overall view (*Figure 4b*), the close up visualized the structural irregularities more precisely (*Figure 4d*). Here, the diagnostically important cement lines were assessed by irregularly arranged formation differing in their diameter and degree of mineralization. Another vertebral detail showed the progressive degree of inadequate mineralization by extensive dark gray areas surrounding the regularly mineralized lamellar bone tissue in the center of the trabecula (*Figure 4e*). However, it was not clear, whether the considerable enlargement of the Havers` systems was the result of a mineralization disturbance (which normally occurs in progressive stages of this disorder) or of a taphonomic process. A few features identified can clearly be linked with post-mortem impacts, such as the vertically oriented fracture line observed within a trabecula (*Figure 4c*) or the structural changes along a small vascular channel of a metatarsal bone (*Figure 4a*).

The pathological manifestations of the Late Antiquity skeleton were in general very similar to the ones identified at the specimen from the PAM collection (*Figures 5c* and *5d*) which was also marked by irregularly formed and mineralized trabeculae with enlarged osteocyte lacunae, distinct cement lines, enlarged and bizarre resorptive surfaces, and indefinite trabecular borders (*Figures 4d* and *5d*). However, the PAM specimen we selected for comparative reason was notable for its less mineralized, but more homogenous appearance. As might be expected, post-mortem alterations were not found (as this preparation was never earth-stored).

DISCUSSION

According to our understanding of the nature of the diseases we are dealing with, it is not surprising that cases of rickets and osteomalacia were rarely described before the 17th century: the risk to develop rickets was generally lower in pre-industrial than industrial communities and individuals predisposed to rickets, e.g., carriers of renal or intestinal dysfunction, are known to have a reduced life expectancy, as already proved by an experimental animal model (Kallay *et al.* 2001). Furthermore, bones of individuals afflicted by rickets or osteomalacia are very fragile. This phenomenon may significantly bias the probability of preservation of ancient remains.

Macroscopic inspection and radiological investigation gave rise to the suspicion that the features observed at the Late Antiquity female skeleton were of osteomalacic origin (Wiltschke-Schrotta, Teschler-Nicola 1991, Teschler-Nicola *et al.* 1996). In particular, the "atypical" fractures and fissures that pertained to cortical bone are widely known symptoms of a mineralization disorder and occur in advanced stages of osteomalacia (*Figures 1b, 1c,* and *1d*). Such fractures are considered an expression of mechanical overstrain at regions of the musculoskeletal system known for their pronounced loading. Gross X-ray analysis confirmed the macroscopical diagnosis by indicating decreased bone density, a coarsened trabecular pattern, and typical radiolucent Looser's zones ("pseudofractures", e.g., on the right scapula and ulna). The latter occurred symmetrical and indicated the Milkman syndrome (*Figure 2c*) – a further characteristic symptom of osteomalacia. In close proximity to the fissures observed radiodense areas were found, representing callus formation as sign of healing (i.e., *Figure 2c*). Thus, the Late Antiquity specimen can be regarded as the first record of osteomalacia (Brickley, Ives 2008) identified in an ancient population of Austria.

To verify this assumption, we compared the specimen with a fluid-conserved vertebra (housed at the osteological collection at the PAM) of an individual with documented osteomalacia: it became clearely apparent that this vertebral body was reduced in its overall dimension (*Figure 5a*). Furthermore, Schmorl's nodes were present. Although the latter indicate heavy work load, the x-ray analysis implied a mineralization disturbance, as there is a broad osteosclerotic region subchondrally visible (*Figure 5b)* – a feature that is described as "Rugger-Jersey-spine" and typically emerges in renal osteodystrophy with an osteomalacic component (Kainberger *et al.* 2003). A differential diagnosis of this historical specimen must consider both, osteopenia and osteoporosis as well. For that reason we extended the technical scope of our study to BSE-mode analysis in SEM as conventional radiography has neither the potential to differentiate clearly between these complex metabolic osteopathies nor to identify minor loss of bone mass (less than 30%; McKenna *et al.* 1987, Kneissel 1993).

BSE-mode analysis in SEM is a well known approach to identify the degree of mineralization and, thus, the inner remodeling activities of bone tissue (Boyde *et al.* 1986, Roschger *et al.* 1995, 2001). But despite its capability, this technique has not yet been applied very often in osteoarcheology (Bell, Jones 1991, Kneissel *et al.* 1994, 1997, Teschler *et al.* 1996 , Brickley et al. 2007).

Although the preservation status of the Late Antiquity skeleton was poor and some of the selected elements were taphonomically changed, the BSE-mode analysis contributed significantly to the diagnosis: we observed differently mineralized bone compartments, but also increased resorption, enlarged osteocyte lacunae with imperfectly mineralized walls, and large amounts of rapidly assembled immature bone (*Figures 4c, 4d,* and *4e*). These features support the previous assumption of osteomalacia.

But beyond that, we identified plexiform bone structures at the scapula (*Figure 3a*), a feature which has up to now never been reported in osteomalacia. It may most likely be a compensatory reaction to achieve better mechanical properties. Martin and Burr (1989) identified this type of bone formation in periods of rapid growth, fracture healing, and in certain diseases (i.e., those associated with increased bone turnover). In addition, we also identified irregular bone arrangements (*Figure 3b*), including small zones of old, regularly mineralized lamellar bone with primary osteons between the lamellae. Secondary osteons – indicators of mature bone tissue – were absent. At the outer trabecular edges parts of newly formed bone were less mineralized (and thus hardly to recover); the latter implies a severe deficiency in calcification. In general, a mineralization disturbance is indicated by the color of the layers – light gray to dark gray reflect the presence respectively the absence of mineral crystals – and by the enlargement of the resorptive lacunae (*Figure 3c*). We also recognized an atypical incidence of primary osteons that were described as "modified vascular channels within lamellae" (Martin, Burr 1989). These structures are the results of sequential bone "filling in" to intracortical vascular channels.

Other cortical areas showed disarrangement as well, e.g., the left tibia (*Figure 3d*) which coincides with the clinical picture of osteomalacia (Teschler-Nicola *et al.* 1996; Schamall *et al.* 2002, 2003b, 2008). The increased endosteal bone resorption and bone formation at the outer layer (*Figure 3e*) is the effect of a remodeling process in reaction to mechanical strains (Ruff *et al.* 2006).

At the fractured and healed metatarsal bone (*Figure 4a*) a normal cortex configuration exists, but adjacent to the former fracture, the compact bone is slightly frayed. This bulked bone is the result of subperiosteal deposition of osteoid, typically followed by a widening and splitting of the cortical contour (Kainberger *et al.* 2003). In contrast, Ortner (2003) stated that subperiosteal deposits do not occur in osteomalacia, but that during the healing of such fractures an internal and external callus is formed that finally mineralizes.

Besides cortical features, cancellous bone changes in vertebrae are of particular diagnostic relevance in the given context. Compared with results obtained on age-related cancellous bone changes (e.g., Kneissel *et al.* 1994, 1997, Foldes *et al.* 1995, Brickley *et al.* 2007), the Late Antiquity specimen undoubtedly shows features that are indicative for increased remodeling and high bone turnover (*Figure 4b*); such incidence is usually linked with an osteoporotic component. Nevertheless, an altered bone turnover is also typical for osteomalacia. While osteoporosis is defined as "*the progressive reduction of amount, thickness and organization of the trabecular network*" (Banse *et al.* 2001, Seeman 2008, Shen *et al.* 2009), osteomalacia results from a general loss of bone mineralization. The latter is the outcome of a failure in calicification of osteoid (osteomalacia therefore belongs to the so-called "*demineralizing osteopathies*" according to Tigges *et al.* 1995, Kainberger *et al.* 2003 and Mays *et al.* 2006): in the course of regular remodeling processes in osteomalacia, newly formed parts of the trabeculae do not mineralize and the hard tissue fraction becomes thin. This phenomenon is depicted very clearly by BSE images as a "thinned trabeculae" (*Figures 4b, 4c,* and *5c*) and complements what is already described by conventional histological sections (e.g., Jaffe 1972). In contrast, osteoporosis results from real thinning of trabeculae till their perforation because resorption dominates over the bone formation.

Despite the widely fragmentary character and a few post-mortem alterations including decomposition and tiny fractures (see *Figures 4a, 4c, 3d* and *4e*), we identified impaired mineralization for the Late Antiquity female by BSE-mode analysis and conclude that she suffered from osteomalacia. As it was not possible to verify this diagnosis by osteoid accumulation (clinically detectable, e.g., by Goldner staining), we compared our findings with the bony microarchitecture of a fluid-conserved vertebral column of a person that is documented in the protocols as being afflicted by osteomalacia (its increased osteoid tissue was approved by Goldner staining, see Schamall *et al.* 2003a). Macroscopically and by X-ray analysis, the PAM specimen shows biconcave vertebrae, a progressive reduction of trabecular structures in the vertebral body center and a coarsened, blurred trabecular network. Besides, sclerotic lines are running parallel to the endplates (*Figure 5b*), which is known as "Rugger-Jersey-Spine" and results from excessive deposition of osteoid (Kainberger *et al.* 2003). Other osteomalacic features in the PAM case are found in the BSE-mode by irregularly formed and mineralized trabeculae, enlarged osteocyte lacunae, and resorptive lacunae (*Figures 5c* and *5d*). The specimen is noteworthy for its less mineralized and homogenous appearance – a criterion that is either related to the high age of the individual or to leaching (the sample had been stored for decades in a preservative agent with unknown composition). Apart from the latter, the changes match the ones observed at the Late Antiquity female and verify the diagnosis of osteomalacia.

It is known that osteomalacia may also be caused by (a) insufficient calcium absorption from the intestine because of lack of dietary calcium (=dietary variant) or (b) a resistance to the action of vitamin D; or (c) Phosphate deficiency evoked by increased renal losses (Revell 1986, Pitt 1995, Löffler, Petrides 2003). Variant "b" can be caused by chronic renal failure, such as renal osteodystrophy (RD), which corresponds to the so-called "Chronic Kidney Disease-Mineral and Bone Disorder" (CKD-MBD, Svára 2009). But it is highly unlikely that vitamin D resistant osteomalacia can be confidently differentiated from the dietary variant in ancient skeletal remains. Nevertheless, there is evidence that the Late Antiquity case was afflicted by osteomalacia without a component of renal insufficiency, whereas the fluid-conserved vertebral body indicates such an involvement (*Table 1*). The very complex pathophysiology and biochemistry

TABLE 1. Differential diagnostic radiological symptoms of renal osteodystrophy observed in the Late Antiquity and historical specimens (+ indicates that this feature is present; – indicates that this feature is not detectable in the skeletal elements; / indicates that this feature cannot be evaluated. The number of algebraic signs points to strength of expression, maximum = +++).

Renal osteodystrophy[1]	Late Antiquity specimen	Fluid conserved specimen
Decreased bone density	++	+++
Thinning of cortices and trabeculae	++	+++
Vertical striations in vertebrae	–	+
"Rugger Jersey" appearance of the vertebral bodies	–	+++
Subperiosteal bone resorption at the phalanges	–	/
Periosteal new bone production (metatarsals, femur, a.o.)	+	/
Loss of definition of the cortical bone	++	+++
Coarsening of the trabecular pattern	++	+++

[1] We selected the features according to Jevtic (2003) and Kainberger et al. (2003); their diagnostic value quality rating is not ascertained.

TABLE 2. Radiological conditions observed among the (five) subforms of renal osteodystrophy (+ indicates that features of this disease are present; – indicates that this pathological condition is not detectable in the skeletal elements. The number of algebraic signs points to strength of association, maximum = +++).

Renal osteodystrophy may lead to skeletal symptoms of	Late Antiquity specimen	Fluid conserved specimen
Osteopenia	++	+++
Osteoporosis	+	++
Osteosclerosis	–	++
Secondary hyperparathyroidism	+	++
Osteomalacia	++	+++

of RD (=CKD–MBD) results in a multitude of clinical pictures, such as osteopenia, osteoporosis, osteosclerosis, secondary hyperparathyroidism, and osteomalacia, which consequently induce a variety of confusing imaging findings (e.g., McKenna *et al.* 1987, Young *et al.* 1991, Formicola 1995, Tigges *et al.* 1995, Jevtic 2003, Kainberger *et al.* 2003, Mankin, Mankin 2008). These findings are discussed in the following.

First, a diminished radiodensity is frequently found in cases of RD. In early stages of RD, osteopenia with moderate loss of bone structure and an increased risk of fractures may occur. As the disease progresses, a more osteoporotic appearance predominates. Excessive resorption of bone generates structural-architectural alterations which then lead to a thinning of the cortical and trabecular compartments, a loss of intertrabecular connections, and biomechanical incompetence (Jevtic 2003, Kainberger *et al.* 2003). In vertebral bodies especially the horizontal trabeculae are resorbed (Thomsen *et al.* 2002), resulting in typical vertical striations of the trabeculae. We found these features in the vertebral bodies of both investigated individuals, but slight manifestations of vertical striations only occurred in the fluid-conserved vertebra.

Second, individuals with RD are afflicted by generalized sclerosis and sclerosis of the bone ends and periosteum (Young *et al.* 1991). However, sclerosis develops not only in patients with RD, but also in individuals afflicted by secondary hyperparathyroidism (sHPT). Most typically, the axial skeleton, in particular the subchondral zones of the vertebral endplates, is involved (Young *et al.* 1991, Jevtic 2003, Kainberger *et al.* 2003). The Late Antiquity individual lacked any osteosclerotic signs, whereas the fluid-conserved specimen showed several radiodense lines below the endplates. Therefore, an osteomalacic condition due to RD and/or sHPT can be deduced for the historical specimen. A sHPT develops due to renal failure which leads to low $1,25(OH)_2D_3$ (= vitamin D), but increased serum phosphate levels. This in turn results in a hypersecretion of parathyroid hormone. Long-term overproduction is responsible for the enlargement of the parathyroid glands and, consequentially, for the development of sHPT (Jevtic 2003) by bone resorption due to increased osteoclastic activity. According to Tigges *et al.* (1995), the first signs of subperiosteal bone resorption appear on the radial aspects of the middle phalanges of the fingers. Following Tigges *et al.* (1995), this location is highly pathognomic. As this feature was not present in our Late Antiquity woman (*Figure 2h*), the diagnosis of sHPT is less likely. But although we failed to find this diagnostically relevant sign in the PAM specimen, the increased osteoclastic activity at the vertebral bodies may indicate such a genesis.

Third, chronic renal dysfunction impairs the kidneys by producing the physiologically active form of $1,25(OH)_2D_3$ which results in an inability to adapt to low dietary calcium intakes that finally leads to a defective mineralization of osteoid (Aufderheide, Rodríguez-Martin 1998). This lack of mineralization is responsible for osteomalacic features by a loss of definition of the cortical bone and a coarsening of the trabecular pattern – signs that were present in both individuals examined.

Summarizing all findings (*Table 2*), the radiological and the BSE-features in the Late Antiquity case correspond well with the ones observed in the fluid-preserved historical specimen, a clinically documented case of osteomalacia,

where we identified features of renal osteopathy and sHPT. The occurrence of RD is, therefore, suggested as the primary etiologic factor with a consecutive development of osteomalacia that was later accompanied by sHPT. Thus, the prior diagnosis of osteomalacia in the Late Antiquity individual (Wiltschke-Schrotta, Teschler-Nicola 1991, Teschler-Nicola *et al.* 1996) can be confirmed by the BSE-mode analysis, which depicted bone tissue of minor quality in the form of unusually and irregularly arranged structures, extended resorption activity, and insufficient bone formation. These features favor the diagnosis of nutritional deficiency of vitamin D and/or calcium in the Late Antiquity specimen. Moreover, we have histological arguments that osteopenia, a mild form of osteoporosis, occurred in this case (evidenced by decreased amount of bone and a thinning of the cortical bone). These metabolic disorders are now regarded as different points along a continuum that can coexist. In contrast, the historical specimen from the PAM showed unquestionable features of osteomalacia, but there are also some structures pointing to the occurrence of RD and sHPT.

ACKNOWLEDGEMENTS

The authors thank Beatrix Patzak for the fluid-conserved specimen of the Federal Pathologic-Anatomical Museum Vienna and appreciate Franz Kainberger who allocated the radiographs. We also extend our gratitude to the Ludwig Boltzmann Institute for Osteology, UKH-Meidling & Hanusch-KH, Vienna, and especially to Paul Roschger for his kind permission to use the BSE-SEM for the Late Antiquity specimen; additionally, we acknowledge the Department of Mineralogy and Petrography, and in particular Franz Brandstätter for producing the BSE-images of the historical case. Furthermore, we gratefully thank Josef Muhsil's and Wolfgang Reichmann's assistance in preparing the graphical work and a suitable layout, and Michaela Kneissel, Hanns Plenk jr., and Christian Reiter for their inputs derived from numerous productive discussions. Finally, we acknowledge two anonymous reviewers for their helpful suggestions.

REFERENCES

ACSÁDI G., NEMESKÉRI J., 1970: *History of Human Life Span and Mortality*. Akadémiai Kiadó, Budapest. 346 pp.

AUFDERHEIDE A. C., RODRÍGUEZ-MARTIN C., 1998: *The Cambridge Encyclopaedia of Human Paleopathology*. Cambridge University Press, Cambridge. 305 pp.

BANSE X., DEVOGELAER J. P., MUNTING E., DELLOYE C., CORNU O., GRYNPAS M., 2001: Inhomogeneity of human vertebral cancellous bone: systematic density and structure patterns inside the vertebral body. *Bone* 28, 5: 563–571.

BELL L. S., JONES S. J., 1991: Macroscopic and microscopic evaluation of archaeological pathological bone: Backscattered electron imaging of putative pagetic bone. *Int. J. Osteoarchaeol.* 1: 179–184.

BOYDE A., MACONNACHIE E., REID S. A., DELLING G., MUNDY G. R., 1986: Scanning electron microscopy in bone pathology: Review of methods, potential and applications. *Scann. Electron. Microsc.* 4: 1537–1554.

BRICKLEY M., MAYS S., IVES R., 2005: Skeletal manifestations of vitamin D deficiency osteomalacia in documented historical collections. *Int. J. Osteoarchaeol.* 15: 389–403.

BRICKLEY M., MAYS S., IVES, R. 2007: An investigation of skeletal indicators of vitamin D deficiency in adults: Effective markers for interpreting past living conditions and pollution levels in 18th and 19th century Birmingham, England. *Am. J. Phys. Anthropol*. 132: 67–79.

BRICKLEY M., IVES R., 2008: *The Bioarchaeology of Metabolic Bone Disease*. Chapter 4. Academic Press, Amsterdam. 41 pp.

BIUKSTRA J. E., UBELAKER D. H., 1994: *Standards for Data Collection from Human Skeletal Remains*. Arkansas Archaeological Survey Research Series Number 44. Arkansas Archaeological Society, Fayetteville. 15 pp.

CARLI-THIELE P., 1996: Spuren von Mangelerkrankungen an steinzeitlichen Kinderskeletten. In: M. Schultz (Ed.): *Fortschritte in der Paläopathologie und Osteoarchäologie*. Band 1, Verlag Erich Goltze, Göttingen.

EINHORN T. A., 1996: Biomechanics of Bone. In: J. P. Bilezikian, L. G. Raisz, G. A. Roda (Eds.): *Principles of Bone Biology*. Chapter 4. Pp. 25–39. Academic Press, San Diego London Boston New York Sydney Tokyo Toronto.

FEREMBACH D., SCHWIDETZKY I., STLOUKAL, M., 1979: Empfehlungen für die Alters- und Geschlechtsdiagnose am Skelett. *Homo* 30, 2: 1–32.

FOLDES A. J., MOSCOVIC, A., POPOVTZER M. M., MOGLE P., URMAN D., ZIAS J., 1995: Extreme osteoporosis in a sixth century skeleton from the Negev dessert. *Int. J. Osteoarchaeol*. 5: 157–162.

FORMICOLA V., 1995: X-linked Hypophosphatemic rickets: A probable Upper Paleolithic case. *Am. J. Phys. Anthropol*. 98: 403–409.

IŞCAN M. Y., KENNEDY K. A. R. (Eds.), 1989: *Reconstruction of Life from the Skeleton*. Alan R Liss Inc, New York.

HOLICK M. F., 2006: Resurrection of vitamin D deficiency and rickets. *J. Clin. Invest*. 116, 8: 2062–2072.

JAFFE H. L., 1972: *Metabolic, Degenerative, and Inflammatory Diseases of Bones and Joints*. Chapter 15. Urban & Schwarzenberg Verlag, München Berlin Wien. 381 pp.

JEVTIC V., 2003: Imaging of renal osteodystrophy. *Eur. J. Radiol.* 46: 85–95.

KAINBERGER F., VASILEVSKA V., KÖLLER M., LERNBASS-WUTZL I., KRESTAN C., GRAMPP S., 2003: Demineralisierende Osteopathien: neue Aspekte der radiologischen Diagnostik. *Wien. Klin. Wochenschr*. 115, 2: 79–86.

KALLAY E., PIETSCHMANN P., TOYOKUNI S., BAJNA E., HAHN P., MAZZUCCO K., BIEGLMAYER C., KATO S., CROSS H. S., 2001: Characterization of a vitamin D receptor knockout mouse as a model of colorectal hyperproliferation and DNA damage. *Carcinogenesis* 22, 9:1429–1435.

KAMBOI M. K., 2007: Metabolic bone disease in adolescents: recognition, evaluation, treatment, and prevention. *Adolesc. Med. State Art Rev*. 18, 1: 24–46.

KNEISSEL M., 1993: *Vergleich von nicht-invasiven und invasiven Methoden zur Erfassung des alters- und geschlechtsabhängigen trabekulären Knochenverlustes an archäologischem Material*. Thesis at the University of Vienna. 10 pp.

KNEISSEL M., BOYDE A., TESCHLER-NICOLA M., KALCHHAUSER G., PLENK J. R. H., 1994: Age and sex-dependent cancellous bone changes in a 4000y BP population. *Bone* 15, 5: 539–545.

KNEISSEL M., ROSCHGER P., STEINER W., SCHAMALL D, KALCHHAUSER G., BOYDE A., TESCHLER-NICOLA M., 1997: Cancellous bone structure in the growing and aging lumbar spine in a historic Nubian population. *Calcif. Tissue Int*. 61: 95–100.

LÖFFLER G., PETRIDES P. E., 2003: *Biochemie und Pathobiochemie*. Springer-Verlag, Berlin Heidelberg New York. 722 pp.

MCKENNA M. J., KLEEREKOPER M., ELLIS B. I., RAO D. S., PARFITT A. M., FRAME B., 1987: Atypical insufficiency fractures confused with looser zones of osteomalacia. *Bone* 8, 2: 71–78.

MANKIN H. J., MANKIN C. J., 2008: Metabolic bone disease: a review and update. *Instr. Course Lect.* 57: 575–593.

MARTIN R. B., BURR D. B., 1989: *Structure, Function, and Adaptation of Compact Bone*. Raven Press, New York. 80 pp.

MAYS S., 2003: The Rise and Fall of Rickets in England. In: P. Murphy, P. E. J. Wiltshire (Eds.): *The Environmental Archaeology of Industry*. Pp. 144–153. Oxbow Books, Oxford.

MAYS S., BRICKLEY M., IVES R., 2006: Skeletal manifestations of rickets in infants and young children in a historic population from England. *Am. J. Phys. Anthropol*. 129: 362–374.

MOLLESON T. I., 1988: Urban bones: The skeletal evidence for environmental change. *Actes 3 Journées Anthropol*., Notes, Mono Techniques 24: 143–158.

MOLLESON T. I., COX M., 1993: *The Spitalfields Project*. Volume 2: The Anthropology. The Middling Sort. Research report. Council for British Archaeology, York. 86 pp.

ORTNER D. J., MAYS S., 1998: Dry-bone manifestations of rickets in infancy and early childhood. *Int. J. Osteoarchaeol*. 8: 45–55.

ORTNER D. J., 2003: *Identification of Pathological Conditions in Human Skeletal Remains.* 2nd Edition. Academic Press, New York. 273 pp.

PITT M. J., 1995: Rickets and Osteomalacia. In: D. Resnick, G. Niwayama (Eds.): *Diagnosis of Bone and Joint Disorders*. Chapter 57. 3rd Edition. Pp. 1885–1920. W.B. Saunders Company, Philadelphia London Toronto.

PLENK JR. H., 1989: Knochengewebe und Zähne. In: P. Böck (Ed.): *Romeis – Mikroskopische Technik*. 17. Auflage. Kapitel 25.3. Pp. 527–566. Urban und Schwarzenberg Verlag, München Wien Baltimore.

REVELL P. A., 1986: *Pathology of Bone*. Chapter 5. Springer Verlag, Berlin Heidelberg New York Tokyo. 113 pp.

ROBERTS C., COX M., 2003: *Health and Disease in Britain: From Prehistory to the Present Day.* Sutton Publishing Ltd, Phoenix Mill Thrupp Stroud Gloucestershire.

ROBERTS C., MANCHESTER K., 2005: *The Archaeology of Disease*. 3rd Edition. Cornell University Press, Ithaca, New York.

ROSCHGER P., PLENK JR. H., KLAUSHOFER K., ESCHBERGER J., 1995: A new scanning electron microscopy approach to the quantification of bone mineral distribution: backscattered electron image grey-levels correlated to calcium Kα-line intensities. *Scanning Microsc. Int*. 9: 75–88.

ROSCHGER P., GRABNER B. M., RINNERTHALER S., TESCH W., KNEISSEL M., BERZLANOVICH A., KLAUSHOFER K., FRATZL P., 2001: Structural development of the mineralized tissue in the human L4 vertebral body. *J. Struct. Biol*. 136: 126–136.

RUFF C., HOLT B., TRINKAUS E., 2006: Who's afraid of the big bad Wolff?: "Wolff's Law" and bone functional adaptations. *Am. J. Phys. Anthropol*. 129: 484–498.

RUFFER M. A., 1911: On Dwarfs and Other Deformed Persons in Ancient Egypt. In: M. A. Ruffer, R. L. Moodie (Eds.): *Studies in the paleopathology of Egypt*. Pp. 35–48. University of Chicago Press, Chicago.

SCHAMALL D., TESCHLER-NICOLA M., KAINBERGER F., TANGL S., BRANDSTÄTTER F., PATZAK B., PLENK JR. H., 2002: Knochenstruktur und Mineralisation in historischem Skelettmaterial mit rachitischen oder osteomalazischen Veränderungen. *Ann. Naturhist. Mus. Wien* 103A: 287–320.

SCHAMALL D., TESCHLER-NICOLA M., KAINBERGER F., TANGL S., BRANDSTÄTTER F., PATZAK B., PLENK JR. H., 2003a: Changes in trabecular bone structures in rickets and osteomalacia – the potential of a medico-historical collection. *Int. J. Osteoarch*. 13: 283–288.

SCHAMALL D., KNEISSEL M., WILTSCHKE-SCHROTTA K., TESCHLER-NICOLA M., 2003b: Bone Structure and Mineralization in a Late Antique Skeleton with Osteomalacia. *Am. J. Phys. Anthrop*. S 36: 184.

SCHAMALL D., 2008: *Qualitative und quantitative Differentialdiagnose von Individuen mit und ohne Mineralisationsstörungen am Beispiel spätantiker, neuzeitlicher und rezenter menschlicher Skelettreste – unter Verwendung des radiologischen, histologischen und histomorphometrischen Analysespektrums*. Thesis at the University of Vienna. 59 pp.

SEEMAN E., 2008: Structural basis of growth-related gain and age-related loss of bone strength. *Rheumatology* 47, Suppl. 4: iv2-iv8.

SIGERIST H. E., 1951: A History of Medicine. Volume 1. *Primitive and Archaic Medicine*. Oxford University Press, New York. 45 pp.

SHEN Y., ZHANG Z.-M., JIANG S.-D., JIANG L.-S., DAI L.-Y, 2009: Postmenopausal women with osteoarthritis and osteoporosis show different ultrastructural characteristics of trabecular bone of the femoral head. *Musculoskeletal Disord.* 10: 35.

SJØVOLD T., 1988: Geschlechtsdiagnose am Skelett. In: R. Knußmann (Ed.): *Anthropologie. Handbuch der vergleichenden Biologie des Menschen*. Band I, 1. Teil. Pp. 446–455. Gustav Fischer Verlag, Stuttgart New York.

STOUT S. D., 1989: Histomorphometric Analysis of human skeletal remains. In: M.Y. Işcan, K. A. R. Kennedy (Eds.): *Reconstruction of Life from the Skeleton*. Pp. 41–52. Alan R Liss Inc., New York.

SVÁRA F., 2009: Chronic kidney disease-mineral and bone disorder (CKD–MBD): a new term for a complex approach. *J. Ren. Care* S 1: 3–6.

STUART-MACADAM P. L., 1989: Nutritional deficiency diseases: A survey of scurvy, rickets, and iron-deficiency anemia. In: M. Y. Işcan, K. A. R. Kennedy (Eds.): *Reconstruction of Life from the Skeleton*. Pp. 201–222. Alan R Liss Inc., New York.

TESCHLER-NICOLA M., KNEISSEL M., SCHAMALL D., WILTSCHKE-SCHROTTA K., 1996: A rare case of osteomalacia in a skeleton from a late antique burial site in Linz, Austria. *J. Paleopathol*. 7: 141.

THOMSEN J. S., EBBESEN E. N., MOSEKILDE L. I., 2002: Age-related differences between thinning of horizontal and vertical trabeculae in human lumbar bone as assesses by a new computerized method. *Bone* 31, 1: 136–142.

TIGGES S., NANCE E. P., CARPENTER W. A., ERB R., 1995: Renal osteodystrophy: imaging findings that mimic those of other diseases. *Am. J. Roentgenol.* 165: 143–148.

WILTSCHKE-SCHROTTA K., TESCHLER-NICOLA M., 1991: *Das spätantike Gräberfeld von Linz / Lentia, Tiefer Graben / Flügelhofgasse*. Linzer Archäologische Forschungen Band 19. Stadtmuseum Linz – Nordico, Linz. 175 pp.

WELLS C. 1964: *Bones, bodies and disease*. Thames and Hudson. London. 288 pp.

YOUNG W., SEVCIK M., TALLROTH K., 1991: Metaphyseal sclerosis in patients with chronic renal failure. *Skeletal Radiol*. 20: 197–200.

ZIVANOVIC S., 1982: *Ancient Diseases. The Elements of Paleopathology*. Pica, New York. 112 pp.

Doris Schamall
Department of Anthropology
Natural History Museum Vienna
Burgring 7
A–1010 Vienna, Austria
E–mail: doris.schamall@nhm-wien.ac.at
Department of Pathophysiology and Allergy Research,
Medical University of Vienna
Waehringer Guertel 18–20
A–1090 Vienna, Austria
E–mail: doris.schamall@meduniwien.ac.at

Maria Teschler-Nicola
Department of Anthropology
Natural History Museum Vienna
Burgring 7
A–1010 Vienna, Austria
E–mail: maria.teschler@nhm-wien.ac.at
Department of Anthropology
University of Vienna
Althanstraße 14
A 1090 Vienna, Austria
E–mail: maria.teschler@univie.ac.at